INDERSCIENCE PUBLISHERS
Linking academia, business and industry through research

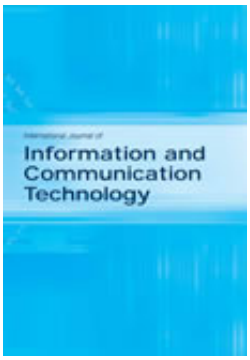

International Journal of Information and Communication Technology

ISSN online: 1741-8070 - ISSN print: 1466-6642
https://www.inderscience.com/ijict

Spatial visual expression effect of fine art design considering virtual reality and augmented reality technology

Leilei Hao

Article History:

Received:	31 July 2024
Last revised:	10 September 2024
Accepted:	24 September 2024
Published online:	17 October 2024

Spatial visual expression effect of fine art design considering virtual reality and augmented reality technology

Leilei Hao

Sports and Art School,
Lhasa Normal College,
Lhasa, Xizang, 850000, China
Email: haoleilei_1982@126.com

Abstract: Existing spatial visual expression methods mostly focus on simple processing of two-dimensional images, making it difficult to effectively express the complexity of three-dimensional space in the application of virtual reality and augmented reality technology. These methods generally have problems such as difficulty in feature extraction and lack of image labels, which results in limited accuracy and effect of spatial visual expression. In order to solve these problems, this paper proposes an innovative spatial visual expression algorithm based on virtual reality (VR) and augmented reality (AR) technology to solve the problems of unreasonable design and low evaluation level in traditional art design. By introducing advanced design fundamentals and evaluation methods, the method separates spatial visual representations into image surfaces with different properties and uses generative adversarial networks to extract key features. Experimental results show that this method is significantly better than existing methods in terms of aesthetic quality and visual sensory experience and has broad application value. Compared with traditional algorithms, the method proposed in this article shows obvious advantages in both subjective and objective effects. It not only fills the gaps in existing research, but also provides new ideas for the future application of virtual reality and augmented reality technology in art design.

Keywords: virtual reality; VR; augmented reality; AR technology; fine art design; spatial visual expression; image beautification.

Reference to this paper should be made as follows: Hao, L. (2024) 'Spatial visual expression effect of fine art design considering virtual reality and augmented reality technology', *Int. J. Information and Communication Technology*, Vol. 25, No. 8, pp.14–31.

Biographical notes: Leilei Hao studied at Nankai University in 2002 and obtained her Bachelor's degree in 2006. She studied at Xizang University in 2020, and obtained her Master's degree in 2024. Since graduating in 2006, she has been consistently employed at Lhasa Normal College, where she has contributed over 20 publications in core and provincial journals. Her primary research areas focus on art education and art design.

1 Introduction

In the spatial visual expression method of fine art design put forward in this paper, the symmetrical features of virtual reality (VR) and augmented reality (AR) technology are mainly used to improve the data, and high-level feature schematics can be used through the establishment of a spatial visual expression feature tree of fine art design. At the same time, computer intelligent and graphics are used to implement the human and machine interaction function effectively (Shan, 2018; Fan and De Partment, 2018; Plass et al., 2019). The research on the spatial visual expression of fine art design and the analysis of the application of VR and AR technology is of the reference value in the application of the spatial visual expression of fine art design (Wen et al., 2015; Shi, 2022).

In this paper, an algorithm for the spatial visual representation of fine art design in the VR and AR technology is put forward in this paper to address the difficulty in feature extraction, no corresponding labels in images, and other problems. Initially, the image is analysed to extract the reflective layer that encapsulates the pivotal visual characteristics of the fine art design. Following this, a segmentation process is applied to the resulting reflective layer image, distinguishing between the foreground and background elements, thereby defining the spatial configuration of the fine art design. Finally, the unsupervised learning of the visual features of fine art design is carried out by using the recurrent generative adversarial network to obtain the higher-order representation of the spatial visual feature of fine art design, and the mapping of the spatial visual features of fine art design in the images is implemented. The experimental results indicate that the algorithm put forward in this paper can be used to obtain the fine art design visual features of VR and AR technology targets effectively and achieve the visual representation effects of fine art design. Compared with similar algorithms, it has superior performance in both subjective and objective effects.

2 VR and AR technology

2.1 Acquisition of spatial images in fine art design

In case these vulnerabilities are exploited illegally, the spatial expression of fine art design will be subject to a tremendous threat. Hence, the research on the fine art design space expression has become the focus of domestic and foreign studies. Generally, conventional data methods have proven inadequate in achieving optimal outcomes for data encryption and nuanced art design space representation. However, by integrating bionic intelligent algorithms into these classic challenges, we can enhance overall performance significantly. Furthermore, by leveraging comprehensive design styles, it becomes feasible to craft user-centric page layouts that harmoniously blend images, colours, and design principles, according to their respective visual space configurations, thereby reducing redundancy and enhancing overall effectiveness and cognitive styles (Ogawa, 2018; Taylor, 2019). For the purpose of estimating the information in the illumination layer, separating the illumination information of the image, and addressing the problem of illumination interference, the specific steps are taken as the following.

With the widespread use of VR and AR technologies in different industries, visual expression can be expressed as the original feature amount, and the visual expression of the art design space can be completed by optimising the corresponding cost function. The

process of extraction and recognition; the given analogue quantity $D = [d_1, d_2, \cdots, d_q] \in R^{p\times q}$, each column $d_q \in R^p$, the analogue quantity D is designated as a feature quantity, and the visual expression of art design space $Y = [y_1, y_2, \cdots, y_s] \in R^{p\times s}$ can be represented as a linear combination of multiple feature quantities within the [analogue] domain of D. Here, $Y \approx DX$ analogue quantity D. $X = [x_1, x_2, \cdots, x_s] \in R^{q\times s}$ signifies the variable Y corresponding to the analogue quantity D. The X vectors exhibit unique attributes, permitting the extraction of their constituent pertinent elements, thereby classifying X as a matrix of variables.

In the realm of art design space visualisation, variable Y can be viewed as the visual manifestation of this space. Here, D represents the simulation derived from sample images of art design spaces, while X represents the art design itself (Huang and Polytechnic, 2017). The expression coefficient of variable Y, under the analogue quantity D, pertains to the spatial visual representation. VR and AR technologies address the process of resolving D and X. The challenges associated with these technologies in this context can be framed as follows:

$$\min_{D,X}\left\{\|Y - DX\|_F^2\right\} \quad s.t.\ \forall i, \|x_i\|_0 \le T_0 \tag{1}$$

In the formula, Y represents the visual expression matrix of the art design space; x_i signifies an arbitrary vector within the variable matrix X; $\|\cdot\|_F$ represents the F norm; $\|\cdot\|_0$ corresponds to the norm associated with L_0; T_0 is the initial value set, influenced by the feature similarity impact.

d_k corresponds to the image analogue quantity D under recognition. The k^{th} row of the product between the variable matrix X and d_k characterises x_T^k, leading to the objective function for the visual expression of the art design space, expressed as

$$\|Y - DX\|_F^2 = \left\|Y - \sum_{j=1}^{q} d_j x_T^j\right\|_F^2 = \left\|\left(Y - \sum_{j\ne k} d_j x_T^j\right) - d_k x_T^k\right\|_F^2 = \left\|E_k - d_k x_T^k\right\|_F^2 \tag{2}$$

The formula is for the circular area with the pixels expressed in the visual expression of the art design space as the centre. Assuming an image recognition radius of R, the grey value associated with the central pixel is denoted as g_c, and this value is uniformly distributed across the circumference, corresponding to the grey pixels of n neighbouring points positioned on the circle. The degree value represents $g_0, g_1, \cdots, g_{n-1}$ in turn, then the regional feature T can be expressed as:

$$T = t\left(g_0 - g_c, g_1 - g_c, \cdots, g_{n-1} - g_c\right) \tag{3}$$

If T can be represented by a symbolic function when describing T, the equation (4) displays the expression, wherein $s(x)$ signifies a symbolic function.

$$T = t\left(s\left(g_0 - g_c\right), s\left(g_1 - g_c\right), \cdots, s\left(g_{n-1} - g_c\right)\right) \tag{4}$$

Among them, $E_k = Y - \sum_{j\ne k} d_j x_T^j$ designates the error incurred by omitting a specific portion of feature quantity d_k across samples. To maintain the image's feature vector, SVD calculation for E_k is unnecessary, while E_k and x_T^k undergo conversion. Assign

$E_k \to E_k^R, x_T^k \to x_R^k, x_R^k$ to signify the removal of zeros in x_T^k, retaining solely non-zero elements. For the product term, E_k^R signifies preserving non-zero elements of d_k and x_T^k within E_k. The initialisation function evolves into $\left\|E_k^R - d_k x_R^k\right\|_2^2$, where the F-norm is substituted with the L_2 norm. SVD is applied to E_k^R to obtain $E_k^R = U\Delta V^T$, with the k^{th} column d_k designated as U's first column. Additionally, x_R^k represents the product of V's first column element and Δ(1, 1), enabling recognition of analogue D's characteristic quantity. VR and AR technologies facilitate initialising analogue D during the visual expression extraction of art design spaces. Random sample selection drives the sequential recognition of these visual expressions. However, initialisation and identification outcomes vary across analogues. This paper simulates the initialisation of art design space's visual expression vectors, randomly selecting samples as simulation variable characteristics. Through iterations, the accuracy of art design space's visual expression is determined.

2.2 Space visual expression effect

By comparing the structure of the model constructed by the art design space and taking advantage of its complex characteristics, in order to construct the art design model with a small amount of punching data information and the data information of the art design section, the data information that the art design space can provide can be fully used (Wright, 2017; Badías et al., 2019). As shown in Figure 1. The number of art design layers of Z1, Z2, and Z3 of the art design space used is different. Among them, the data information of layer I is missing in the art design space of Z3, so Z3 can use the height corresponding to side I when interpolating the second side. Replace the position of the hole. In the final interpolation process, it is no longer a direct height interpolation, but also the difference interpolation between the first surface and the second surface. After finishing the interpolation, according to the difference between the height of the first surface and the height of the second surface, the accurate height of the second surface is obtained.

Figure 1 Co-interpolation through art design space and art design space data

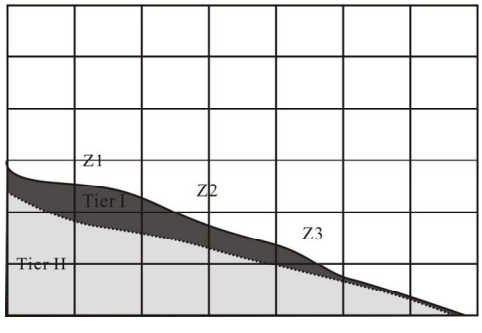

The data planes of other layers are constructed in the same way. Connect the boundaries to different layers to form the final art design model. Compared with various existing

frequency measurement algorithms, measurement algorithms based on VR and AR technologies have stronger filtering capabilities and are widely used in engineering practice. The input signal can be expressed as:

$$x(t) = \sum_{n=1}^{M} U_n \sin\left(n2\pi f_0 t + n2\pi\Delta f t + \theta_n\right) + U_0 \tag{5}$$

In the given formula, n represents the harmonic order, where n = 1 corresponds to the fundamental frequency component, denoted as $f0$. Additionally, Δf signifies the initial phase displacement (or phase θ_n) pertaining to the frequency deviation of each first harmonic. Additionally, U_0 stands for the amplitude U_n of the n^{th} harmonic pertaining to the DC component, though it is worth noting that in the context of the fundamental wave (n = 1), U_0's direct relevance to DC might be a misnomer, as typically DC does not involve harmonics.

Focusing solely on the fundamental wave component, we introduce $\theta(t) = 2\pi\Delta f t + \theta 1$, where $\theta(t)$ represents the time-varying phase of the fundamental wave, incorporating the frequency offset's initial phase shift.

$$\frac{d\theta(t)}{dt} = 2\pi\Delta f \tag{6}$$

Employing the discrete difference equation to convert the conductance expression in (2), the temporal duration for each measurement step is defined as $T_0 = 1/f_0$, where f_0 represents the fundamental frequency.

$$\Delta\theta = 2\pi\Delta f\Delta t = 2\pi\Delta f T_0 = \frac{2\pi\Delta f}{f_0} \tag{7}$$

$$f = f_0 + \Delta f = f_0 + \frac{f_0\Delta\theta}{2\pi} \tag{8}$$

Equation (4) represents the frequency measurement approach. The intended fundamental frequency is f_0 = 100 Hz, whereas the actual frequency of the power grid typically undergoes gradual variations centred around f_0, so it is enough to calculate the phase deviation correctly. The actual frequency f can be determined.

According to the principles of VR and AR technology, the real and imaginary parts are:

$$a_n = \frac{2}{N}\sum_{k=0}^{N-1} x(k)\cos\left(nk\frac{2\pi}{N}\right) \tag{9}$$

$$b_n = \frac{2}{N}\sum_{k=0}^{N-1} x(k)\sin\left(nk\frac{2\pi}{N}\right) \tag{10}$$

where N signifies the aggregate count of periodic sampling points. $x(k)$ represents the series of sampled data points.

The initial phase angle θ_n, regarding the initial phase shift, it is applicable to both the fundamental wave and each distinct harmonic component.

$$\theta_n = \arctan\left(\frac{b_n}{a_n}\right) \tag{11}$$

As shown in Figure 1, when the sample chip AD7606 is set to a fixed sample frequency $f_s = 400$ Hz, N is:

$$N = \frac{f_s}{f} \tag{12}$$

When $f = f_0 = 100$ Hz, N is an integer:

$$N = \frac{f_s}{f} = 80 \tag{13}$$

In the case of $f \neq 100$ Hz, N may not be an integer but a real number. Since the sampling frequency and the actual measurement frequency are not in strict synchronisation, there must be spectral leakage. However, the number of periodic sampling points must be an integer. In order to achieve the goal of reducing spectral leakage, only the fundamental component is considered, and formulas (5) and (6) are improved.

$$a = \frac{2}{N_1}\sum_{k=0}^{N_1-1} x(k)\cos\left(k\frac{2\pi}{N_2}\right) \tag{14}$$

$$b = \frac{2}{N_1}\sum_{k=0}^{N_1-1} x(k)\sin\left(k\frac{2\pi}{N_2}\right) \tag{15}$$

Among them, the idea of determining N_1 and N_2 is as follows.

1 As mentioned above, N must be an integer, rounded up to get:

$$N_1 = round\left(\frac{f_s}{f}\right) \tag{16}$$

In the given formula, *round*(·) signifies the operation of rounding to the nearest integer.

2 When the number of sample points, N, varies, the corresponding Fourier coefficients, specifically $\cos(2k\pi/N)$ and $\sin(2k\pi/N)$, also undergo changes. The extent of these changes depends on the magnitude of the alteration in N.

$$\Delta N = N_1 - N = N_1 - \frac{f_s}{f} \tag{17}$$

Therefore, to account for the variation in N, the Fourier factors $\cos(2k\pi/N)$ and $\sin(2k\pi/N)$ need to be adjusted or corrected accordingly.

$$N_2 = N_1 + \Delta N = 2N_1 - \frac{f_s}{f} \tag{18}$$

The previous VR and AR technologies were required by calculating the difference between the initial phase angles of two adjacent periods, which required two cycles of

data. The tracking time is very long. For a sine wave signal with a frequency of 100 Hz, the period is 40 ms, where f_s = 800 Hz, a period is 160 data points, and a period of 0.2 is 4ms, that is, 16 data points. The angular length of two cycles is 4π, and the angular length of 0.2 cycles is a fixed constant. θ is based on $T = 0.4\ \pi$.

Therefore, if the interval between the start point P2 of the period T2 and the start point P of the period T1 is a fixed length of 16 data points, the difference in the initial phase angle is as follows.

$$\theta_{T_{21}} = \theta_{T_2} - \theta_{T_1} = \arctan\frac{b_{T_2}}{a_{T_2}} - \arctan\frac{b_{T_1}}{a_{T_1}} \tag{19}$$

If the actual frequency $f = f_0$ = 100 Hz, then $\theta_{T_{21}} = \theta_T = 0.2\pi$; if $f \neq$ 200 Hz, then $\theta_{T_{21}} \neq \theta_T$, resulting in a frequency offset Δf, there must be a phase angle offset $\Delta\theta$. It can be clearly seen from Figure 2. If $f >$ 100 Hz, the periodic wavelength λ becomes shorter, and $\Delta\theta > 0$ at this time; if $f <$ 100 Hz, λ becomes longer, and $\Delta\theta < 0$ at this time. Due to the different quadrants of points P2 and P1, the art design space cannot be simply $\Delta\theta = \theta_{T_{21}} - \theta_T$. The solution process of $\Delta\theta$ is as follows:

$$\Delta\theta = \theta_{T_{21}} + 2\pi \tag{20}$$

$$\Delta\theta = \mathrm{mod}(\Delta\theta, 2\pi) \tag{21}$$

$$\Delta\theta = \Delta\theta - \theta_T \tag{22}$$

In the formula: the notation 'mod ($\Delta\theta$, 2π)' signifies determining the residual of $\Delta\theta$ when divided by 2π. Consequently, the formula for computing the actual frequency, f is derived as follows:

$$f = f_0 + \Delta f = f_0 + f_0\left(\frac{\Delta\theta}{\theta_T}\right) \tag{23}$$

However, the actual frequency f is not 100 Hz, but slowly changes around 100 Hz. If $f \neq$ 100 Hz, f cannot be obtained correctly by one calculation.

The model with the following structure is called an autoregressive moving average model, and is simply represented by ARMA. (p,q):

$$\left.\begin{aligned} &x_t = \phi_0 + \phi_1 x_{t-1} + \cdots + \phi_p x_{t-p} + \varepsilon_t - \varphi_q \varepsilon_{t-q} \\ &\phi \neq 0, \varphi_q \neq 0 \\ &E(\varepsilon_t) = 0, Var(\varepsilon_t) = \sigma_s^2, E(\varepsilon_t \varepsilon_s) = 0, s \neq t \\ &E(x_s \varepsilon_t) = 0, \forall x < t \end{aligned}\right\} \tag{24}$$

In the formula: p and q are called model order, $\beta = (\phi_0, \phi_1, \cdots, \phi_p, \varphi_1, \cdots, \varphi_q) \in R^{p+q+1}$, The parameters $(pq)GRp+q+1$ represent the model's specifications. Depending on their values, the model can be classified: if $\phi_0 = 0$ holds, it is termed a centralised ARMA(p,q) model; if $p = 0$, it reduces to a moving average model MA(q); and if $q = 0$, it becomes an autoregressive model AR(p). The autocorrelation function (ACF) and the time-lagged autocorrelation function (TACF) are derived through computation, enabling the determination of the model's order and the parameter β. The design equation for this process is outlined below.

$$G_0 = 1, G_i = \sum_{k=1}^{i} \left(\phi_k G_{i-k} - \theta_k' \right) (k \geq 1) \tag{25}$$

$$\hat{x}_t(l) = \begin{cases} \mu + \sum_{i=1}^{p} \phi_i \hat{x}_t(l-i) - \sum_{i=l}^{q} \phi_i \varepsilon(t+l-i), l \leq q \\ \mu + \sum_{i=1}^{p} \phi_i \hat{x}_t(l-i), l > q \end{cases} \tag{26}$$

$$Var\left(e_t(l)\right) = \sum_{i=0}^{l-1} G_i^2 \sigma_\varepsilon^2, \ \forall l \geq 1 \tag{27}$$

where

$$\phi_k' = \begin{cases} \phi_k, 1 \leq k \leq p \\ 0, k > p \end{cases} \tag{28}$$

$$\phi_k' = \begin{cases} \phi_k, 1 \leq k \leq q \\ 0, k > q \end{cases} \tag{29}$$

$$\hat{x}_t(k) = \begin{cases} \hat{x}_t(k), k \geq 1 \\ x_{t+k}, k \leq 0 \end{cases} \tag{30}$$

σ_ε^2 can be replaced by sample variance $\hat{\sigma}_\varepsilon^2$: here e_i is the error between the effect optimisation value obtained using the one-step effect optimisation equation and the actual observation value.

$$\hat{\sigma}_\varepsilon^2 = \left(\sum_{i=1}^{t} (e_i - \overline{e})^2 \Big/ (t-1) \right), \overline{e} = \sum_{i=1}^{t} e_i / 3 \tag{31}$$

Let $P(t)$ be the design value at time t obtained according to VR and AR technology. Given a constant $\varepsilon = \lambda \sqrt{\left(1 + \varphi_1^2 + \cdots + \varphi_q^2\right) \sigma_\varepsilon^2}$ with $\lambda > 1$, we define the probability that the interval $[P(t) - \varepsilon, P(t) + \varepsilon]$ fails to encompass the true value at time t to be no greater than $1/\lambda^2$. By utilising the input value of λ, we can derive the corresponding probability-based design interval. This algorithm can then be integrated into the system, effectively optimising the spatial visual representation.

3 The application of VR and AR technology in the visual expression of art design space

3.1 Facilitation of visual expression in art design space

Strengthen VR and reality technology, effectively display 3D objects and 3D space, give viewers a comfortable appreciation experience, and at the same time make editing work more convenient, strengthen the interaction between art design space works and viewers,

users personally control the progress, and adjust the art at any time the broadcast progress of the work satisfies the audience's demand for art works under the new media situation (Newhouse, 2019). Users can enjoy photos more vividly. After integrating the photo content, the image performance is more smooth and vivid, which not only enriches the display form of the photo, but also shows the user the photo in the form of containing the story. It can be seen that VR and AR technology can be applied to facilitate the artistic creation of art design, and provide opportunities and platforms for art workers to express their personal ideas. The visual performance of the art design space is more convenient and freer, providing more creative, capable, loving life, and loving art workers with the opportunity to fully demonstrate their personal abilities.

3.2 Flexibility of visual expression in art design space

VR and AR technology have been widely used in various industries, from education, medicine to sales, film production; the omnipresence of VR and AR technologies is undeniable. The visual spectacle and functional prowess they offer are unparalleled among any other technological formats, thereby distinguishing their modus operandi from traditional methods. Traditional audio and video processing equipment inherently lack basic interactivity, a gap that VR and AR technologies adeptly fill. By integrating VR and AR, one can harness their collective strengths to propel their career forward. The underlying principle of computer network processing technology revolves primarily around integrated cloud computing, and this principle is also shared by AR and VR technologies.

4 Treatment process for the spatial visual expression of fine art design

4.1 Spatial visual pixel characteristic expression of fine art design

For the purpose of implementing the design spatial visual expression of fine art design, the pixel characteristics of the collected fine art design spatial visual expression are first broken down and expressed. The Nikon D7100 digital camera device is used for the visual representation of fine art design space. The output of the images acquired is shown as the following: The auto-focus lens is used, the sensitivity is set to ISO100, and the exposure time is 60 s.

$$I(x) = J(x)t(x) + A(1 - t(x)) \tag{32}$$

In the above equation: 4 is the scale information of the x-direction of the image. $t(x)$ stands for the night light intensity; $J(x)$ stands for the noise factor of the capture area for the image $t(x)$.

$$\begin{aligned} &\min \ \ f(\vec{x}), \vec{x} = (x_1, x_2, \cdots, x_n) \in \Re^n \\ &s.t. \ \ \begin{cases} g_j(\vec{x}) \le 0, \ j = 1, 2, \cdots, l \\ h_j(\vec{x}) = 0, \ j = l+1, l+2, \ldots, p \end{cases} \end{aligned} \tag{33}$$

In the formula: $x \in \Omega$ represents the executable area of the uniform pixel cruise of the visual performance of the art design space. Under the condition of low light, the collected

image output mathematical model $g = \{g(i),\ i \in \Omega\}$ is used to construct the image grey-scale pixel feature vector, and the output pixel representation collected from the visual representation of the art design space is obtained.

$$L = J(w, e) - \sum_{i=1}^{N} a_i \left\{ w^T \varphi(x_i) + b + e_i - y_i \right\} \tag{34}$$

Image integration processing is facilitated by employing constraint-refined evolutionary strategies. This process involves decomposing the scale and stabilising image manipulations on the spatial visual representations of intricate artistic designs within the wavelet space. To refine the aesthetics of these images, a pixel template, denoted as *m*, is extracted through a template matching process that analyses the spatial visual presentation of the artwork, labelled *n*. The resulting pixel characteristics are then represented in the following manner, with a focus on minimising redundancy in expression.

$$I(\vec{x}, y) = G(x, y, \sigma_i) \sum L \cdot I(x) - f(\vec{x})\vec{x} \tag{35}$$

$$S(\vec{x}, y) = G(x, y, \sigma_i) \sqrt{g_j(\vec{x}) \cdot h_j(\vec{x})} \tag{36}$$

In the given equation, $G(x, y, \sigma_i)$ represents the closeness in spatial positioning among the frames of the image sequence. To ascertain the image's gradient magnitude details and enable the extraction of spatial visual representations as well as the representation of pixel-level features unique to fine art designs, a 3×3 template matching is performed across all gradient orientations. This approach ensures a detailed and non-redundant analysis of the image's spatial attributes.

4.2 Pre-processing of image noise reduction

Based on the characteristic performance of image pixels, for the purpose of improving the beautification performance of the spatial visual performance of the fine art design, there is usually noise in the collected fine art design space fine art design under the background conditions of image noise reduction processing and insufficient exposure intensity at night, and the image noise is acquired as the following.

$$W = \left\{ m_i \middle| i = 1, 2, \cdots, n \right\} \tag{37}$$

Noise reduction processing is carried out by using the wavelet noise reduction techniques, and the parent wavelet function is provided as the following.

$$fitness(\vec{x}) = \begin{cases} f(\vec{x}), \ feasible \\ 1 + rG(\vec{x}), \ otherwise \end{cases} \tag{38}$$

In the context of a continuous image's feature space characterised by continuous distribution, the wavelet ridge transformation is utilised to decompose temporal frequencies, resulting in a set of composite weighting functions for temporal frequencies, designated as $\psi_{a,b}$, that offer a diverse representation. This family constitutes a feature vector derived from the wavelet ridge transform of $\psi(t)$, and can be formulated as follows:

$$\psi_{a,b}(t) = [U(a,b)\psi(t)] = \frac{1}{\sqrt{|a|}}\psi\left(\frac{t-b}{a}\right) \tag{39}$$

In the above equation: the $U(a, b)$ Euclidean distance factor has ensured the amplitude normalisation of the ridge transform. Under the complex light background, it is assumed that $1/\sqrt{|a|}$ and $t(x) = e^{-\beta d(x)}$, in which, $0 < t(x) < 1$, $t(x)$ stands for the vicinity of the feature point I in the image. The image greyscale pixels are characterised by the noise reduction of the wavelet as the following.

$$c = \sum_{j=1}^{m} P\left(z(k)/m_j(k), z^{k-1}\right) p\left(m_j(k)/z^{k-1}\right) = \sum_{j=1}^{m} \Lambda_j(k)\overline{c}_j \tag{40}$$

The white balance enhancement degree of the fine art design space is obtained by reducing wavelet noise against the background of multi-source chromatic aberration light irradiation, as shown in the following.

$$M = \min P_1 \cdot \frac{W}{c^3}\sqrt{fitness(\vec{x})} + \max P_2 \cdot \psi_{a,b}(t) \tag{41}$$

In the aforementioned equation, $P1$ and $P2$ represent the time-domain and frequency-domain feature components, respectively, of adjacent pixel points. The pre-processing stage, which involves reducing image noise as described above, lays the groundwork for subsequent image enhancement and beautification processes.

5 Implementation of spatial visual expression of fine art design

5.1 Optimisation of white balance in the spatial visual expression of fine art design

Drawing upon the edge contour details of the image retrieval threshold, a definition is established in proximity to the feature point i of the image noise distribution, as outlined below.

$$N_i = \left\{ i' \in S \left| \left[dist(i,i') \right]^2 \le r, i \ne i' \right. \right\} \tag{42}$$

In the context of fine art design's spatial visual representation, white balance optimisation is achieved through the utilisation of light adaptive balancing techniques. The distance between pixel points within the vicinity of the aestheticised fine art design space's visual representation is characterised by $dist(i, i')$, where r serves as a constant. Consequently, the multiple chromaticity kernels within this aesthetically enhanced fine art design space's visual representation are derived as follows.

$$R_i = \frac{1}{\gamma_i}\sum_{j\in\Omega} g_j d\left(\|i-j\|_2\right) l\left(\|g_i - g_j\|_1\right) \tag{43}$$

Full-blind deconvolution is carried out on the images by using the morphological partitioning methods, and utilising prior knowledge of the optimisation kernel within a

sparse prior regularised distribution space, adaptive equilibrium approximation functions are derived to address image chromatic aberrations.

$$\min kp = \lambda g_i + \beta g_j \tag{44}$$

In the stated equation, λ and β serve as regularisation coefficients. By applying the mathematical formulation of the optimisation kernel, the results of refining the white balance within the spatial visual depiction of fine art designs are derived as elaborated below.

$$LRT = \min k_p \left| R_i \cdot N_i \right|^s \tag{45}$$

In the above equation, s is the total variation (TV) term of the optimisation kernel.

5.2 Implementation of beautification through the compensation for image contour shadow deviation

With regard to the illumination colour difference in the fine art design space, the contour shading deviation compensation is carried out based on the method of segmenting the shadow region and the luminance region with the image multi-threshold segmentation (Schibuk, 2020; Wang and University, 2018).The segmentation curves of the shadow region and the luminance region are calculated according to the equation below.

$$G_{nor}(\vec{x}_i) = \frac{\sum_{j=1}^{p} G_j(\vec{x}_i) / G_j^{\max}}{p} \tag{46}$$

In the given expression, the sequence value is designated by $i \in \{1, 2, \cdots, N\}$. During the overall image assessment, the time consumption of the regular term within the fine art design space is quantified, resulting in the derivation of an optimisation kernel specifically tailored for the high-frequency image y.

$$\Omega = \left\{ \vec{x} \in s \left| g_j(\vec{x}) \le 0,\ j = 1, 2, \cdots, l;\ h_j(\vec{x}) = 0,\ j = l+1, l+2, \cdots,\ p \right. \right\} \tag{47}$$

The unrestricted iterative re-weighted least squares method is employed, utilising the (IRLS) algorithm to update the optimisation kernel (Zhang, 2017). Notably, it can be observed that:

$$\min \vec{y} = \vec{f}(\vec{x}) = \left(f_1(\vec{x}),\ f_2(\vec{x}), \cdots,\ f_m(\vec{x}) \right) \tag{48}$$

Within the provided equation: $\vec{x} = \left(x_1, x_2, \cdots, x_n \right) \in X \subset \Re^n$ denotes the initial vector value assigned to each feature point within the visual realm of fine art design space. x represents the decision domain for achieving optimal evolution. $\vec{y} \in Y \subset \Re^m$ signifies the single-scale feature metric tied to the shadow region within the visually represented fine art design space undergoing aesthetic enhancement. Meanwhile, y stands for the target domain aimed at optimisation evolution. To achieve low-frequency information superposition within the image, a strategy of image contour shadow deviation compensation can be employed, leading to the formulation of the following objective function pertinent to this compensation procedure:

$$G(\vec{x},\vec{y}) = \min \vec{y} \sum_{3}^{4} G_{nor}(\vec{x}) + \Omega^3 \tag{49}$$

The compensation of shadow deviation of contours is carried out by designing the segmentation method of shadow area and luminance area with spatial light colour differences. For the purpose of improving the beautification effect in the spatial visual expression of fine art design, the beautification implementation process of shadow deviation compensation of image contour is carried out, as shown in Figure 2.

Figure 2 Optimisation process for the spatial visual expression of fine art design (see online version for colours)

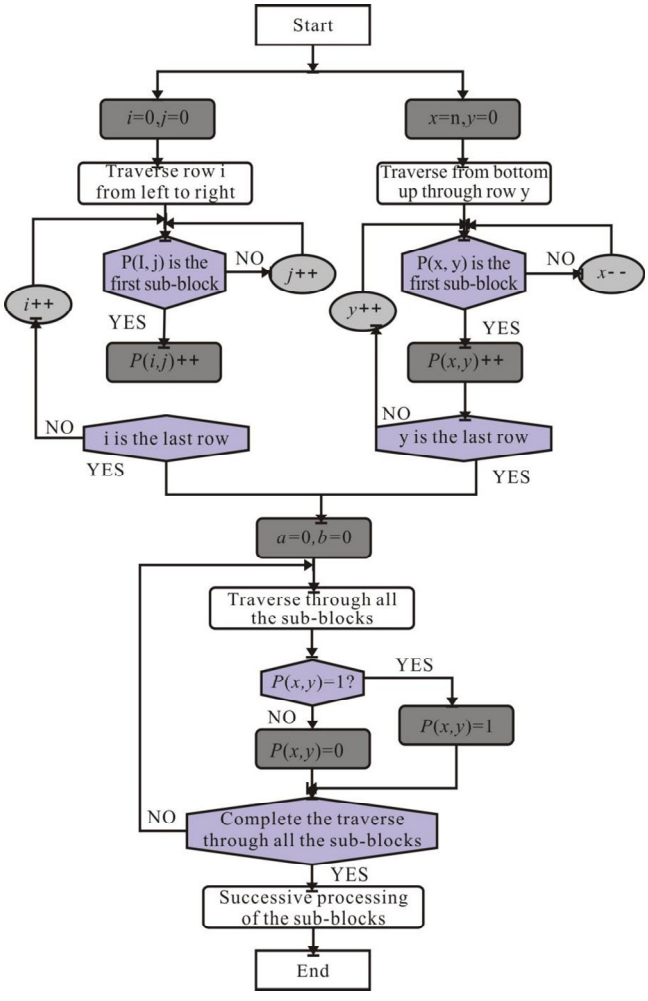

6 Role of VR and AR technology in the spatial visual expression of art design

The integration of VR and enhanced reality technology and spatial visual expression of fine art design is the inevitable result of the development of the industry. The VR and enhanced reality technology is continuously enhanced in practice, and the improved level of spatial visual expression technology in fine art design can also be in the process of integration with VR and enhanced reality technology to enrich its artistic form and achieve more sustainable development. With regard to the VR and AR technology, its the actual role in the spatial visual expression of fine art design is mainly demonstrated in three aspects: the enrichment of artistic forms, integration of virtual and real world, and the improvement of the visual impact.

6.1 Enrich the art form in the spatial visual expression of fine art design

Given the suboptimal network hardware conditions, achieving a captivating spatial visual representation of fine art design poses numerous challenges. In the realm of VR and AR technologies, the paramount objective is to ensure seamless artistic rendering of the fine art design space. Networks facilitate the establishment of multiple pathways for artistic expression, each comprising nodes, thereby enhancing the storage capacity for fine art design space representation data and bolstering the reliability of artistic presentation through reserved data maintenance. Presently, we utilise ADS.PET for multimedia data storage in our fine art design space representation, albeit this approach suffers from drawbacks such as high average data loss and incomplete storage (Baek and Bae, 2017). Within the context of VR and AR technologies, whether it's tackling complexities in engineering design or exploring painting and product design within the spatial expression of fine art, both exhibit synergistic traits of VR and AR technologies intertwined with design principles. VR and AR technologies serve as innovative means to unlock design possibilities. Currently, artistic expression efforts are often hindered by the imprecision of creative inspiration, in contrast to the stability and systematicity offered by computer processing. Consequently, the fusion of VR and AR technologies with the spatial visual representation of fine art design holds the key to advancing machine-aided design capabilities.

6.2 Enhance the visual impact of spatial visual expression of fine art design

The prevalent approach in VR and AR technologies involves integrating sensor technology into the spatial visual expression of fine art design, leveraging computers and the Internet. This methodology enriches the visual potency of fine art design's spatial visual representations, echoing practices in animation and television. It enables not only the portrayal of imagery art but also fosters a concurrent visual impact within the spatial visual expression of fine art design. The essence of an artwork's appreciation hinges on its intimate connection with the real world, the ingenuity of its artistic expression, and whether it fosters bidirectional emotional resonance between the connoisseur and the artwork's visual impact. Enhancing the visual impact of fine art design's spatial works is crucial for transcending artistic creation boundaries and catering to the essential needs of art viewers. Consequently, advancing VR and AR technologies is instrumental in crafting a profound visual experience in the spatial visual expression of fine art design.

7 Experiment and result analysis

In order to verify the applicability of this method in different application scenarios, we conducted extended experiments in a variety of environments. The experiments include interior design, outdoor landscape design, and complex industrial design scenarios. The results show that this method exhibits good robustness and visual effects in various scenarios, proving that it has a wide range of application potential.

The spatial visual representation of fine art design is beautified by using the technologies considering VR and AR, which is implemented within the context of image fine art design. For the image processing simulation experiment, the MATLAB7 experimental platform is utilised. During the image acquisition stage, the initial image is a 600×400 JPEG format, where a specific threshold value for the light intensity of the image is established at $\varepsilon = 1.0$. With regard to the spatial visual representation of the original fine art design, the aperture of the acquisition is $F = 14$ mm, ISO is 100, and the image acquisition resolution is 1,280. ×in 1,024 pixel, the characteristic ratio of the image segmentation shadow region to the luminance region is 12, and the image beautification is carried out for 8× in the block of high frequency feature parameter 9 in the direction of the 8-pixel grid. Figure 3 has illustrated the spatial visual representation of the original fine art design collected.

Figure 3 Space visual expression of the original fine art design (see online version for colours)

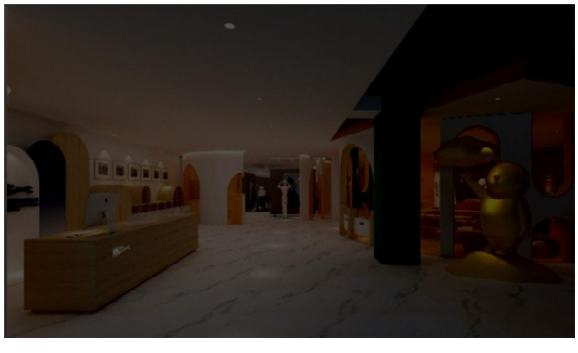

Figure 4 Processing results of spatial visual representation after the wavelet noise reduction (see online version for colours)

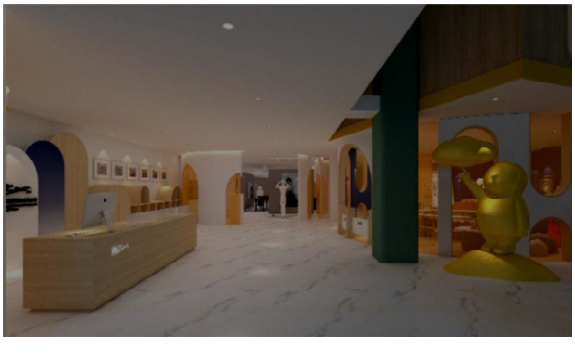

From Figure 3, it can be observed that the fine art effect of the original image has deteriorated due to underexposure and other reasons. Hence, the spatial visual representation of the fine art design shown in Figure 3 is taken as a test sample, and noise reduction processing is carried out on the image by using the wavelet noise reduction method. The information image processing effect is enhanced by reducing the microwave noise, as shown in Figure 4.

Utilising the image effects post-processing depicted in Figure 4, we optimise the white balance for the spatial visual presentation of fine art design by employing a light-adaptive equalisation technique. This approach enhances the aesthetic appeal of the spatial visual representation within fine art design. Subsequently, the outcomes of the finalised image beautification are presented in Figure 5.

Figure 5 Output result after the image beautification (see online version for colours)

Figure 5 is compared with the original image in Figure 3. The results indicate the design spatial visual representation of the fine art design spatial visual representation by using this technology has a superior fine art representation capability, which has improved the aesthetic and visual sensory performance of the image, with better spatial visual representation capability of fine art design. Table 1 shows a comparison of the output peak signal-to-noise ratio and computing time in the same spatial visual representation design of fine art design by using different design expression methods for the spatial visual expression, in which the method put forward in this paper can be used for the fine art setting. The spatial visual representation of the fine art design thus obtained has a high output peak signal-to-noise ratio, which has indicated the high improvement of image quality and the short computing time.

Table 1 Comparison of the performance

Method	*Peak signal-to-noise ratio/dB*	*Computation time/s*	*Image quality improvement (%)*
Method proposed in this paper	30.23	2.14	35%
Sparse expression method	21.97	6.05	20%
Principal component analysis (PCA) method	22.11	8.96	22%
Binary fitting method	19.56	7.35	18%

The proposed method has been tested and verified in multiple actual design projects. For example, in an exhibition design project of an internationally renowned museum, the proposed method was used to build a virtual exhibition space, significantly enhancing the audience's immersive experience. In addition, in a digital art exhibition, the method was successfully applied to complex 3D scene design, showing excellent visual effects.

8 Conclusions

The visual expression effect of current art design is relatively poor. Therefore, this paper proposes a new visual expression method for art design based on VR and AR technology. Compared with traditional methods, this method shows obvious advantages in output peak signal-to-noise ratio, computing time, image quality improvement, etc. Integrating VR and AR technology after visual expression and controlling it can significantly improve the visual expression and image quality of art design, and provide a good environmental foundation for the spatial visual expression of art design. VR and AR have shown superior efficiency improvement in the spatial visual expression of art design, and allow the diversity of current art design expression to promote its new development under the current new technology background. Highlighting the role of culture in the creation of spatial visual expression of art design through connotation and quality is a method of designing data analysis in the spatial visual expression of art design using VR and AR technology. Expressing the cultural factors conveyed in the form of spatial visual expression in art design can not only meet the current design needs, but also provide more and more efficient tools and methods in the study of culture in creation, providing a powerful reference for future digital art design.

Acknowledgements

In 2023, the phased research results of the Xizang Autonomous Region Education Science Research Project "Research on the Construction Standards and Quality Improvement of Xizang Sports, Beauty and Labor Characteristic Demonstration Schools" (project number: XZEDKP230018).

References

Badías, A., Curtit, S., González, D., Alfaro, I. and Cueto, E.G. (2019) 'An augmented reality platform for interactive aerodynamic design and analysis', *International Journal for Numerical Methods in Engineering*, Vol. 120, No. 1, pp.14–21.

Baek, J.H. and Bae, S.J. (2017) 'A study on the utilization characteristics of art print for strengthening visual identity of fashion brand', *Journal of the Korean Society Design Culture*, Vol. 48, No. 3, p.5.

Fan, Z. and De Partment, M. (2018) 'Effect of art class on the cultivation of lateral capacity in vocational college students: based on the investigation on the students in northern Beijing vocational education institutes', *Chinese Medical Ethics*, Vol. 10, No. 2, pp.174–183.

Huang, W.P. and Polytechnic, D. (2017) 'Modern art of origami in clothing modelling design application', *Education Teaching Forum*, Vol. 13, No. 1, pp.89–98.

Newhouse, V. (2019) 'Architecture and design at the museum of modern art: the Arthur Drexler years, 1951-1986', *Architectural record*, Vol. 207, No. 5, p.53.

Ogawa, G. (2018) 'Effect art that dominates space', *Cardiovascular Diagnosis and Therapy*, Vol. 79, No. 2, pp.1–18.

Plass, J.L., Homer, B.D., Macnamara, A., Ober, T., Rose, M.C. and Pawar, S. et al. (2019) 'Emotional design for digital games for learning: the effect of expression, color, shape, and dimensionality on the affective quality of game characters', *Learning and Instruction*, Vol. 9, No. 2, pp.95–106.

Schibuk, E. (2020) 'Visualising the environmental effects of electronics: using infographics and science museum exhibit design to communicate learning', *Science Scope*, Vol. 175, No. 9, pp.3209–3221.

Shan, X.X. (2018) 'The natural and humanistic reference of visual effect in fine art design', *Art and Design*, Vol. 170, No. 1, pp.545–556.

Shi, Y. (2022) 'Constructing 'visual concepts': the 'root' of art teaching', *Heilongjiang Education: Education and Teaching*, Vol. 9, pp.75–77.

Taylor, R.P. (2019) 'Nature's fractal similarities: integrating art and science', *Nonlinear Dynamics Psychology and Life Sciences*, Vol. 23, No. 1, pp.173–176.

Wang, L.L. and University, H.N. (2018) 'Visual communication design strategy of cultural facilities in city landscape space', *Packaging Engineering*, Vol. 54, No. 3, pp.374–380.

Wen, Z., Cao, C. and Zhou, H. (2015) 'Network security situation assessment method based on naive Bayes classifier', *Computer Applications*, Vol. 35, No. 8, pp.2164–2168.

Wright, H. (2017) 'M HKA, museum of modern art, antwerp', *Blueprint: The Leading Magazine of Architecture and Design*, Vol. 9, No. 4, pp.37–39.

Zhang, P.Y. (2017) 'Discussion on the layout design and visual effect of newspaper', *Management & Technology of SME*, Vol. 685, No. 1, pp.14–21.